



LAWRENCE
LIVERMORE
NATIONAL
LABORATORY

Engineering Precision Relocation Capability Into A Large-Cantilevered Telescoping Diagnostic for a Kirkpatrick-Baez X-Ray Optic

M. J. Ayers, L. A. Pickworth, T. Decker, R. Hill, T. Pardini, T. McCarville, N. Shingleton, C. Smith, C. G. Bailey, P. M. Bell, D. K. Bradley, N. F. Brejnholt, S. Hau-Riege, M. Pivovarovoff, P. B. Mirkarim, M. Vitalich, J. Vogel, C. Walton, J. Kilkenny

August 19, 2014

SPIE Optics + Photonics 2014
San Diego, CA, United States
August 17, 2014 through August 20, 2014

Disclaimer

This document was prepared as an account of work sponsored by an agency of the United States government. Neither the United States government nor Lawrence Livermore National Security, LLC, nor any of their employees makes any warranty, expressed or implied, or assumes any legal liability or responsibility for the accuracy, completeness, or usefulness of any information, apparatus, product, or process disclosed, or represents that its use would not infringe privately owned rights. Reference herein to any specific commercial product, process, or service by trade name, trademark, manufacturer, or otherwise does not necessarily constitute or imply its endorsement, recommendation, or favoring by the United States government or Lawrence Livermore National Security, LLC. The views and opinions of authors expressed herein do not necessarily state or reflect those of the United States government or Lawrence Livermore National Security, LLC, and shall not be used for advertising or product endorsement purposes.

ENGINEERING PRECISION RELOCATION CAPABILITY INTO A LARGE-CANTILEVERED TELESCOPING DIAGNOSTIC FOR A KIRKPATRICK-BAEZ X-RAY OPTIC

M.J. Ayers¹, L. A. Pickworth¹, T. Decker¹, R. Hill¹, T. Pardini¹, T. McCarville¹, N. Shingleton¹, C. Smith¹, C. G. Bailey¹, P. M. Bell¹, D. K. Bradley¹, N. F. Brejnholt¹, S. Hau-Riege¹, M. Pivovarov¹, P. B. Mirkarimi¹, M. Vitalich¹, J. Vogel¹, C. Walton¹ and J. Kilkenny²

1. Lawrence Livermore National Laboratory, Livermore CA

2. General Atomics, San Diego CA

ABSTRACT

The Kirkpatrick Baez Optic (KBO) diagnostic designed for the National Ignition Facility (NIF) requires very precise alignment between four pairs of mirrors that make up four x-ray imaging channels. Furthermore, the overlapping image axis of the four pairs must be aligned to within a 50 μm radius of the NIF target center. In order to achieve this the diagnostic utilizes a telescoping snout that when extended, locates the mirrors at the end of a Diagnostic Load Package (DLP), cantilevered more than three meters out from its bolted connection points. Discussed in this paper are the structural challenges and the mechanical design solutions that were implemented to achieve the $\pm 50 \mu\text{m}$ pointing accuracy. During an Inertial Confinement Fusion (ICF) experiment, the KBO diagnostic will be 117 mm away from the extremely high impulse, target implosion shock wave, which requires a unique approach to protecting the sensitive optics which will also be discussed.

Keywords: x-ray imager, x-ray optics, Kirkpatrick Baez, multi-layer, diagnostic load package, NIF, DLP, GXD

1. INTRODUCTION

Time gated x-ray imaging¹ is essential for experiments at the National Ignition Facility (NIF)². It provides temporally resolved images that are used for measuring shape, size and burn history of an imploding cryogenic deuterium-tritium (DT) capsule as it is compressed during Inertial Confinement Fusion (ICF) experiments. To further study the symmetry and fuel size during implosions new time resolved x-ray imaging capabilities are required. The most heavily utilized x-ray imaging systems at NIF are the pinhole array framing cameras. The pinhole array projects a large number of x-ray images onto a micro channel plate (MCP) and allow spectral filtering and debris protection through the use of thin film filters. The temporal gating of the MCP (~ 100 ps exposure per image from a voltage ramp across two or four ~ 250 ps strips which can be independently triggered) captures the x-ray images at different times in the implosion, reconstructing a temporal history of the capsules shape, size and burn history. Gated x-ray imaging with an array of pinholes is foundational, but has limitations that include pinhole diameter limited resolution and throughput, and limited ability for chromatic selection. A method to address these limitations is to use grazing incidence x-ray optics. This addresses the need for higher resolution, throughput and, via the application of a multilayer coating, narrow energy bandwidth imaging. The current design of this new x-ray microscope will provide improved resolution (better than $10 \mu\text{m}$ half-power diameter); 4.5x greater throughput when compared to similar pinhole imaging systems; and selectable bandwidths, using four KB channels that relay four images to the detector.

2. GENERAL SYSTEM OVERVIEW

2.1 Kirkpatrick-Baez (KB) x-ray optical system

A Kirkpatrick-Baez x-ray imaging system or optic (KBO) consists of two grazing incidence mirrors positioned at right angles to each other such that a 2D x-ray image is formed. The system is described fully in reference³ and the optimization of a KB system for high resolution and throughput is described fully in reference⁴. NIF will use a microscope setup with high magnification, i.e. larger than 10.5x. As the KB uses grazing incidence mirrors, multilayer coatings can be developed for the operational incidence angle that allows a ~ 1 keV band centered at an energy defined by the experiment. The large collection angle of KB systems allows a single image to be the

equivalent in signal strength of many pinhole images but with a pseudo monochromatic spectral content. KBO systems have been fielded at other laser facilities with great success^{5, 6}, and some of these systems have also used depth graded multilayer mirrors to archive narrow band x-ray images⁷. The NIF KBO, shown in Figure 1, will initially work at 10.2 keV⁸ with an exchangeable mirror pack design that allows the energy response of the mirrors to be matched to the experiment. The mirror pack will contain 4 KB channels which image onto a time gated detector with >10.5x magnification (Magnification in the x-y axis of the image is different due to the offset in the two mirror centers). Achieving this high throughput and magnification requires placing the diagnostic within 117 mm from the ICF target; this close proximity required a unique engineering design to protect the sensitive mirrors.

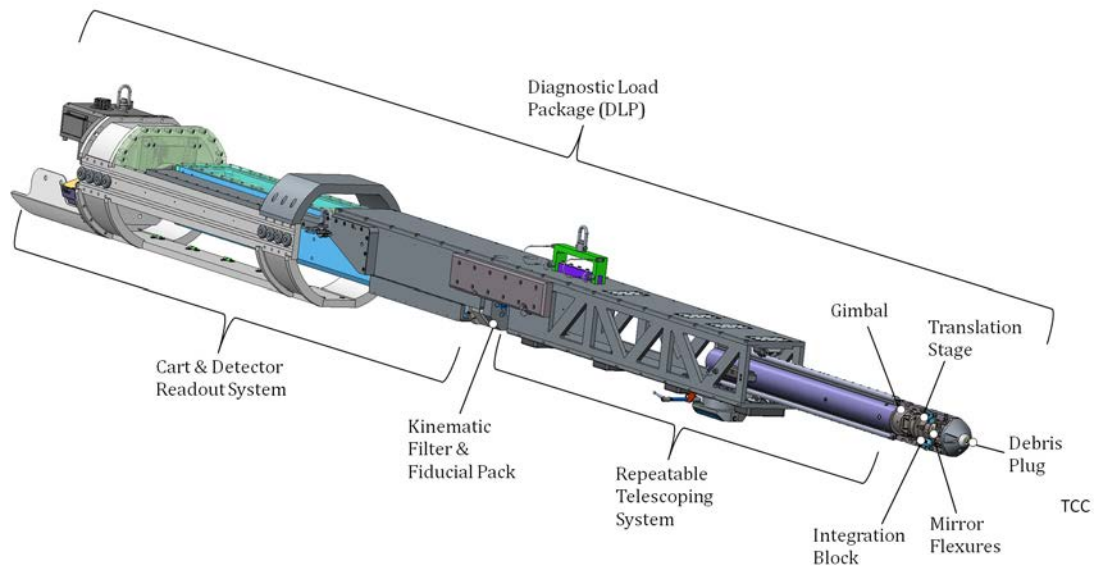


Figure 1. KBO x-ray microscope diagnostic load package (DLP) for use in a diagnostic instrument manipulator DIM on the National Ignition Facility (NIF).

2.2 Overview of the components in the NIF KBO system

There are multiple components that make up the KBO. These are shown in the overview in Figure 1. Starting from the right hand side at target chamber center (TCC), the diagram shows the debris window, precision engineered mirror flexures for mounting and alignment of the KB mirrors, an integration block which combines the 4 imaging channels, a translation stage and gimbal which houses a pinhole array behind the KB mirrors. This comprises the debris shroud and mirror pack which mate to the repeatable telescoping snout via a kinematic base mounting.

The repeatable telescoping snout also houses a cross over block, not shown in Figure 1 that contains a slot that allows the pinhole images to pass to an image plate, but blocks the direct line of sight to TCC for each of the four KBO images. These components are shown from the side in Figure 2 (top panel), along with an exploded view of all active imaging components (bottom panel).

At the detector plane a kinematic filter/fiducial pack (the image plate holder shown in Figure 2) is located 8 cm in front of the micro-channel plate that captures the KBO images. The pinhole images are recorded on an image plate held in the kinematic filter/fiducial pack and provide additional spectral and pointing data for the first deployment of the KBO. Both the filter pack and the crossover block provide additional shielding to line of sight neutrons and high-energy x-ray that increase the noise and background in the MCP image.

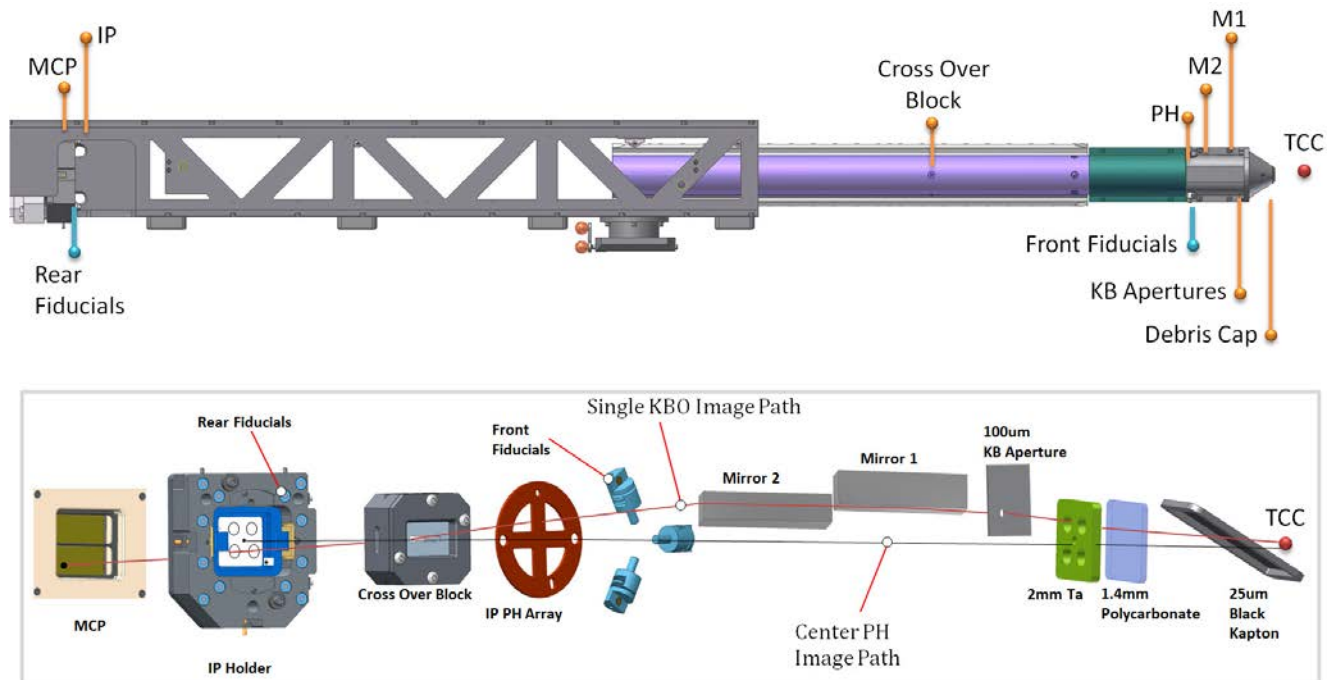


Figure 2. Imaging path for the four KB images and the pinhole images.

The KBO will work with existing x-ray gated detector technology¹, initially using electronic CCD readout capable of collecting data at yields up to $Y_n \sim 10^{14}$ with ~ 100 ps exposure per image. Future iterations will use film readout and be capable of capturing data at higher yields⁹ up to $Y_n \sim 10^{17}$. The length of the air box, 1 m, used to house the x-ray framing camera constrains the usable length of the DLP, further motivating the use of a highly repeatable telescoping section to position the KBO mirror pack. The air box for the gated x-ray detector (GXD) is mounted inside a cart with an attached box tube that provides the rail mountings for the repeatable telescoping portion of the snout.

In order to improve the alignment of the diagnostic a second set of alignment fiducials is added at the kinematic filter/fiducial pack in addition to the alignment fiducials on the mirror pack itself, shown in Figure 2. This will allow the DLP to be pointed to TCC to better than $\pm 50 \mu\text{m}$ via the NIF Opposing Port Alignment System (OPAS)¹⁰.

2.2.1 KBO Optical Path

In this section we will follow the optical path of the four KB images back to the imaging plane. This perspective is shown to help tie all the pieces together that have been described thus far. Refer to Figure 2 for the following description. The optical path of the four KB images begins by passing through the debris plug, which consists of the two plastic filters shown and an apertured plate: firstly passing through the $25 \mu\text{m}$ thick black kapton ablative shield, then through the primary debris shield that consists of 1.4 mm of polycarbonate and through an oversized aperture machined into a 2 mm thick Ta support structure that sits directly behind the polycarbonate. The two 30 mm long x 6.5 mm wide KB mirrors receive the incoming signal through a $100 \mu\text{m}$ diameter aperture which limits the illuminated surface of the mirror to $\sim 1/3$. This increases the pointing tolerance of the mirror, sets the incidence angle and improves the resolution. Following this the signal is reflected off the multilayer on mirrors 1 and 2, then through the open apertures of the image plate pinhole array. The four incoming images cross at the 1.3 cm thick heavy-met crossover block and pass through the filter and image plate holder. The filters and image plate in the IP holder are apertured for each of the four KB images, ~ 9 mm diameter, to prevent overlap and further reduce background contribution at the detector. Finally the KB image is collected on the MCP and read out via a charge-coupled device (CCD).

3. ASSEMBLY AND ALIGNMENT

3.1 Achieving high alignment tolerance in a DIM based DLP

The KBO has a limited field of view ($\sim 300\text{ }\mu\text{m}$) requiring a stricter alignment tolerance than the standard $\pm 250\text{ }\mu\text{m}$ to target. Tighter alignment capability has been achieved on other equatorial DIMs using a front and rear fiducial set¹¹; these systems formed the basis for the alignment system in the KBO. The optimization of the NIF KBO for detector-limited resolution at the center of the field of view is described in Reference 8. Resolution is a key deliverable of the diagnostic, and as such the assembly and alignment tolerance are driven by their impact on the overall resolution delivered at the edge of a $50\text{ }\mu\text{m}$ diameter object. In order to achieve the stated resolution of the diagnostic (better than $10\text{ }\mu\text{m}$ FWHM) the optical axis of the KB imaging system must be pointed within a $\pm 50\text{ }\mu\text{m}$ radius of the target.

The contribution of pointing and assembly error into achieving this resolution can be summarized in the error contributions from the following systems: (1) Assembly and alignment of the mirror pack, which deviates the optic response from the ideal, (2) assembly of the mirror pack into the DLP, (3) repeatability of the extendable boom and (4) the accuracy of the NIF alignment systems and the NIF target positioning systems. Figure 3 illustrates this metric of pointing tolerance, showing the degradation of the optical performance by expected assembly and optic quality tolerances against the effect of misalignment to a target center. It is seen that the alignment is the largest source of degradation for the optic performance.

The following section will discuss the engineering solutions applied to the KBO assembly to achieve the stated resolution of the diagnostic.

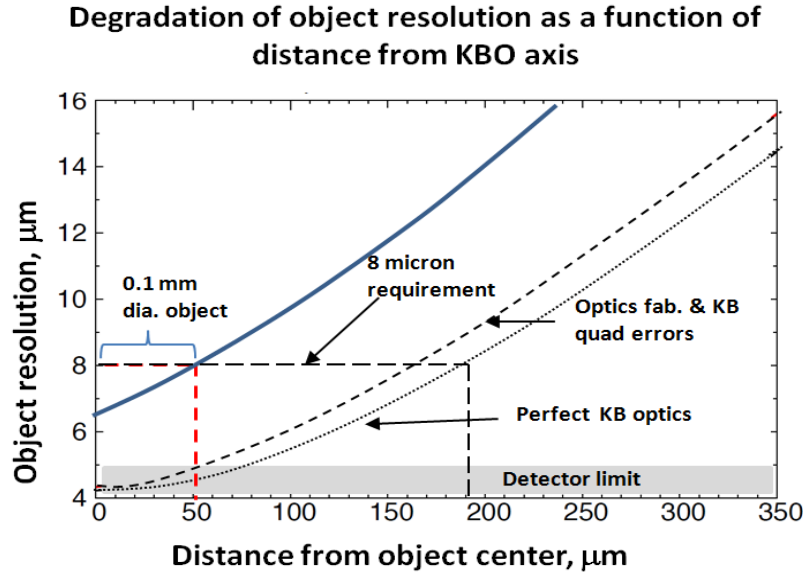


Figure 3: Using the resolution at the edge of a $50\text{ }\mu\text{m}$ radius as a metric for alignment performance, this graph demonstrates the expected impact on ideal alignment (dotted line), due to expected error in mirror pack assembly (dashed line) and error in alignment to target (solid blue line). The origin of the x-axis represents the center of the object being imaged⁸.

3.2 Assembly and alignment of Mirror pack

Figure 4 shows the key components of the mirror pack assembly. This contains all the imaging components of the DLP and is designed to be a single unit assembled together with the alignment fiducials that can be exchanged without disrupting the snout alignment. This subsection will discuss the assembly and alignment of a mirror pack that was primarily designed and implemented by T. Decker and R. Hill.

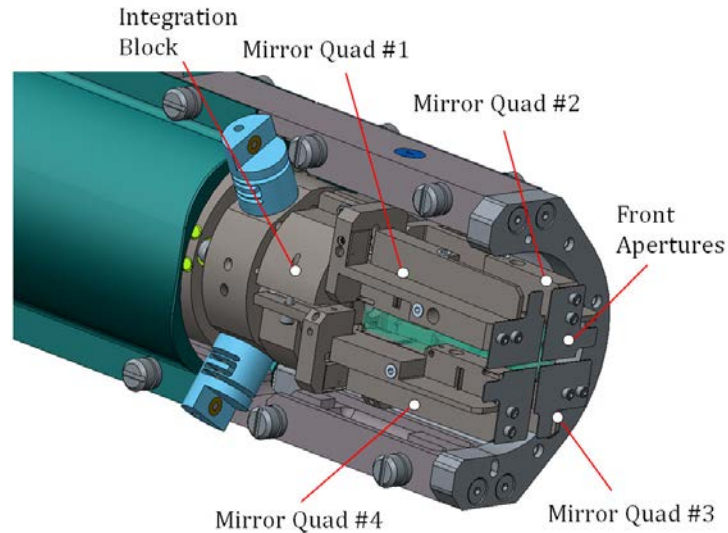


Figure 4. Front of KBO snout with cone and shields removed. All four channels shown including front apertures that provide a single image of the target for each mirror pair.

3.2.1 Mirror Quad assembly using a Coordinate Measuring Machine (CMM)

In order to meet requirements in alignment the mirror pack is assembled on a coordinate measuring machine. This provides the benefit of a high accuracy common coordinate system in which the mirrors and their fixtures can be jointly located. This allows the pitch for each mirror to be precisely set, $\pm 80 \mu\text{rad}$, and the mirrors to be positioned within $2 \mu\text{m}$ of their ideal locations with respect to each other. The positioning of the aperture on each imaging channel can be performed with high accuracy after the mirrors are aligned using the optical system on the CMM. The CMM alignment of the mirror pack will also correctly position the OPAS alignment fiducials as well as the pinhole plate.

3.2.2 Integration block, Translation stage and Gimbal

One of the key advantages of the x-ray microscope over current pinhole imaging is the ability to select specific energies. A flow-down requirement for this capability is that the mirror packs be exchangeable while installed in a DIM. This is particularly challenging because there is no opportunity to verify alignment of the system between mirror pack exchanges. An optical master target that shares the same absolute tooling ball locations as the mirror pack defines the coordinate system used to align the mirror pack. The key to making this system work is a master alignment fixture that locates the three kinematic tooling balls in the same positions on the master target and the KBO mirror pack, (Figure 5). The coordinate system on the CMM is defined by using the optical component of the CMM and the master target. Once the coordinate system has been defined the master target is removed and the mirror pack put in its place. The master target now becomes the alignment standard and is also used to align the KBO DLP. Each mirror pair and its respective quad are co-aligned on the CMM to the coordinate system defined by the master target.

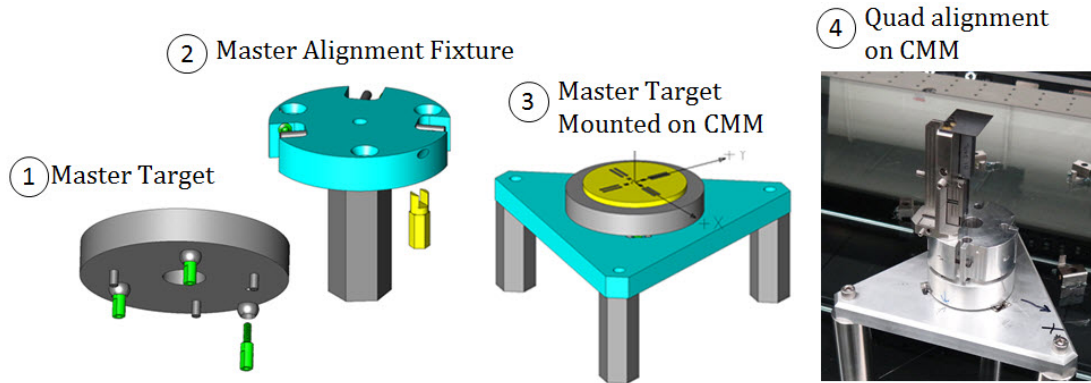


Figure 5. (1) Master target used to define coordinate system on CMM. (2) Master alignment fixture used to replicate position of tooling balls on master target and all mirror packs. (3) Master target mounted on kinematic base used to create coordinate system on CMM. (4) Actual quad on CMM for alignment.

This concept ensures each mirror pack is looking at the same point in space with respect to the z-axis defined by the master target on the kinematic mount. Verification of the repeatability of the kinematic mount system can be obtained using an off-line x-ray source and measuring the image shift at the detector¹² induced by coupling and decoupling of the kinematic mount.

Before beginning alignment of the KB quads there are two prior alignment processes that are carried out. First a flexure mounted in the center bore of the integration block containing a pinhole array is aligned. The center pinhole array is aligned using the optical CMM. The second step is to align the front set of OPAS targets, shown in Figure 6. Alignment in the target chamber with OPAS uses three high contrast targets located on the perimeter of the integration block and a set back at the detector plane, set in the “IP holder” marked in Figure 2 and shown in Figure 14. By making the two sets of targets concentric to each other and aligning the centroid of each set through TCC, $\pm 50 \mu\text{m}$ pointing can be achieved using OPAS. The high contrast targets on the integration block are mounted on flexures so that they can be adjusted radially to an equal distance from the center axis defined by the CMM.

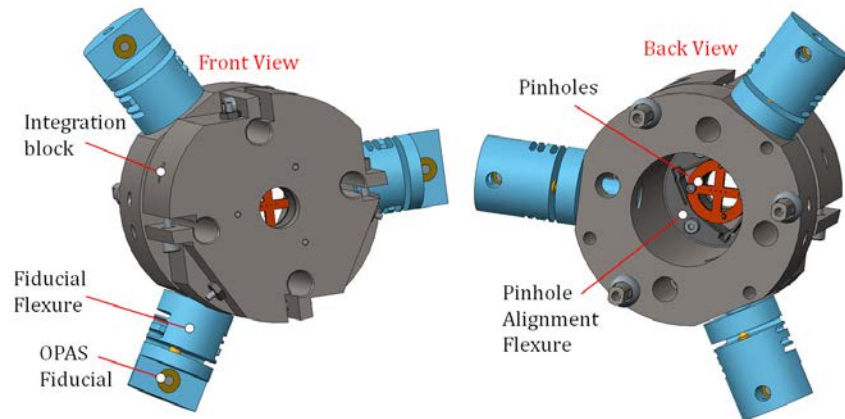


Figure 6. Pinhole array mounted on a flexure inside the integration block. The pinhole array is used to provide alignment data and baseline imaging for comparison of x-ray optic data. Data is collected on image plate in a filter pack (IP holder) on the front of the gated x-ray detector. Fiducials for OPAS are adjusted to an equal distance from center axis for alignment in the TC.

3.2.3 Mirror Flexures

The mirror pairs are mounted to four precision-engineered Ti6Al4V flexures, shown in Figure 7. The parallax angle between the 4 lines of sight was minimized by mounting the mirror pairs in a tightly packed manner, whilst allowing the required degrees of freedom of the optics to be adjusted.

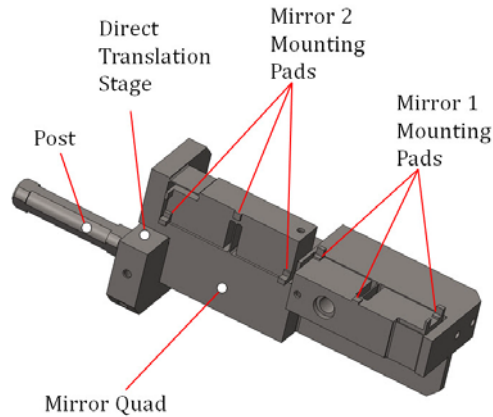


Figure 7. Individual precision engineered titanium mirror quad prior to optics bonding.

The mirror pairs are bonded to the quad mount on machined features that exactly constrain the optics relative to each other. A set of parallel flexure blades for each optic allows precise pitch adjustment. At the base of the quad is an additional set of parallel blade flexures that allow translation adjustment of the quad to $\pm 2 \mu\text{m}$ from the center axis of the optical system. The gross angle of the mirror pair is set by mounting the post, marked in Figure 7, into the quad mounting locations, marked in Figure 8, which are precision bored at the required incidence angle for the mirror, 0.6° .

3.2.4 Mirror quad and Aperture placement

The four quads are then inserted into the integration block in the precision machined bores set at 0.6° off the center axis, rotated into position and clamped in place by the post. The four mirror pairs are shown mounted into the integration block in Figure 8.

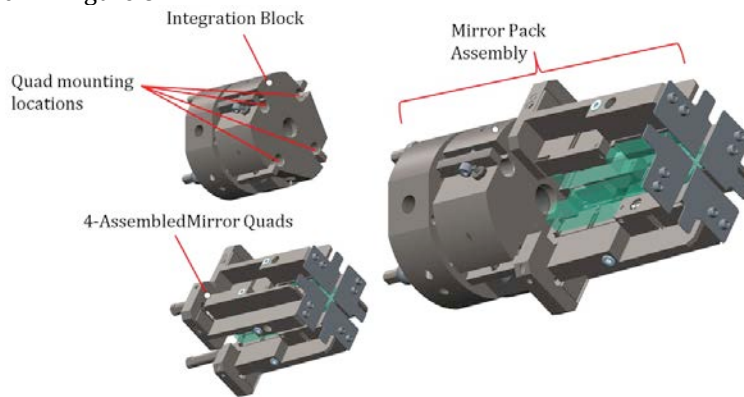


Figure 8. All four channels of the KBO assembled with optics and aligned to the integration block using CMM. One quad has been removed from the right hand image for clarity.

Each optic is then pitched into the correct position and translated to the proper offset from the center optical axis. This process is repeated for each of the four quads. Next the quads are rotated to the proper orientation, locked down by the post clamp and the final location of the optics is verified as a final step. Following this the $100 \mu\text{m}$ aperture plates are installed onto the front of the quad using the optical system of the CMM, Figure 9. To verify successful alignment each individual quad is then measured using an off line 1.5 keV x-ray source. The measured resolution of one assembled KBO quad fit the predicted model indicating the optics are well aligned¹². A conceptual plan to measure the resolution and co-alignment of all four quads simultaneously has been developed¹².

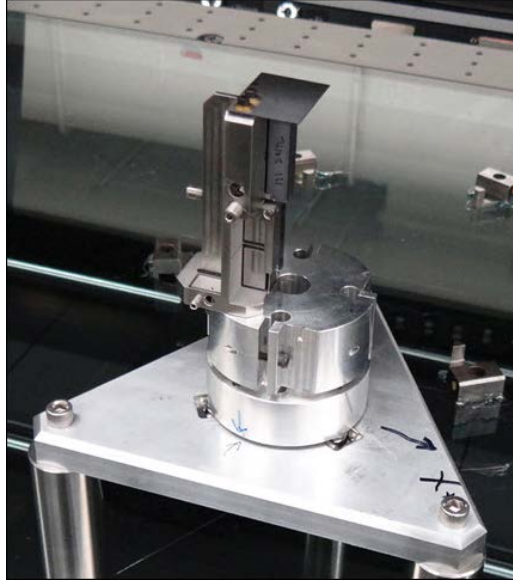


Figure 9. Image of aperture alignment as it is performed on the CMM.

3.3 Telescoping Snout and Box tube assembly

3.3.1 Overview of the snout build

The NIF KBO x-ray microscope is designed to be fielded in a NIF diagnostic instrument manipulator (DIM)13. The fielding of the first system will be deployed on the equatorial target chamber DIM ports 90-78 and 90-315, designated by their θ and ϕ in spherical coordinates. Space limitations within the NIF facility did not allow for a one-piece construction of the KBO diagnostic support structure. Figure 10 illustrates the loading scenario for a Diagnostic Load Package (DLP), in which the DLP must pivot between the target bay wall and the access door of the DIM. The space available between the target bay wall and the rear access door of the DIM is the limiting dimension for the overall length of the KBO diagnostic. The physics requirements dictate that during operation the mirror pack is positioned 181mm (center of first mirror) from target chamber center (TCC), and the detector positioned 2436mm from TCC. To meet the required magnification and still fit behind the DIM the KBO design required an integral 1m telescoping section to shorten its overall length. When collapsed the KBO system can be transported using standard diagnostic handling units (DHU) and loaded into the DIM using standard protocols and procedures.

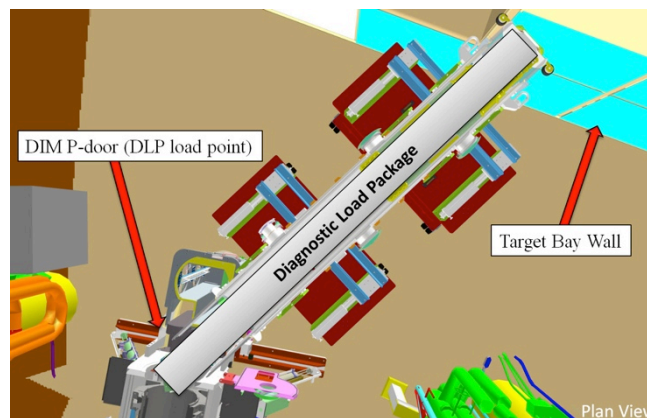


Figure 10. KBO x-ray microscope diagnostic load package (DLP) positioned behind the DIM, overall length is limited by clearance between the target bay wall and DIM rear access door.

3.3.2 The Telescoping snout

One of the many challenging constraints in developing the KBO x-ray microscope was the space limitation for diagnostic load package (DLP) transport and installation into the diagnostic instrument manipulator (DIM). To obtain the required $>10.5\times$ magnification of the system the overall length of the DLP grossly exceeded the allowable footprint. It was chosen to implement a telescoping section that could be retracted during transport and installation as this would meet the alignment requirements for the KBO. The telescoping design would need to withstand the shock from the debris wind, rare seismic events and be repeatable in position to within $20\text{ }\mu\text{rad}$ between shots. The design chosen was an extendable boom guided by a set of linear rails. The rails are constrained by sets of precision ABEC7 radial bearings separated by 90° spread about the two opposing linear rails, Figure 11. A preload device is used to load the boom into the upper bearing set as well as define its insertion depth where it rests in a detent machined into the lower rail. The preload device is a lobed shaft or cam mechanism that applies an upward force when rotated. As the preload device is rotated a center piston fitted with radial bearings at either end ride up the ramp on the lobe. The upper bearing loads against the bottom rail, as the distance between the lower rail and the lobe on the shaft become shorter the shaft deflects acting like a spring, Figure 12. A manual spring-loaded plunger is used to lock the telescoping boom in either the retracted, transport, maintenance or the extended position. The bearing packs that carry the load when the boom is extended are all fixed, the remaining bearing packs are spring-loaded and have compliance for the boom to smoothly retract.

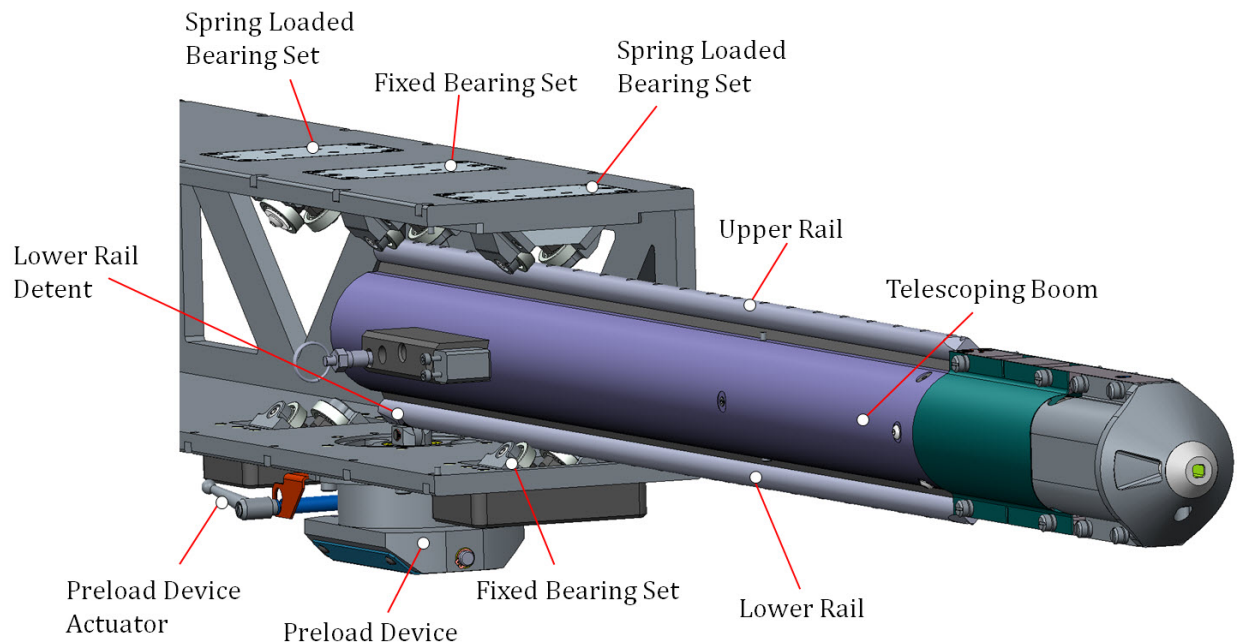


Figure 11. Shown are the primary components of the 1 m telescoping boom used for the KBO. The boom is constrained by two fixed sets of precision bearings and a pre-load device. The nearest wall of the box structure has been removed for clarity.

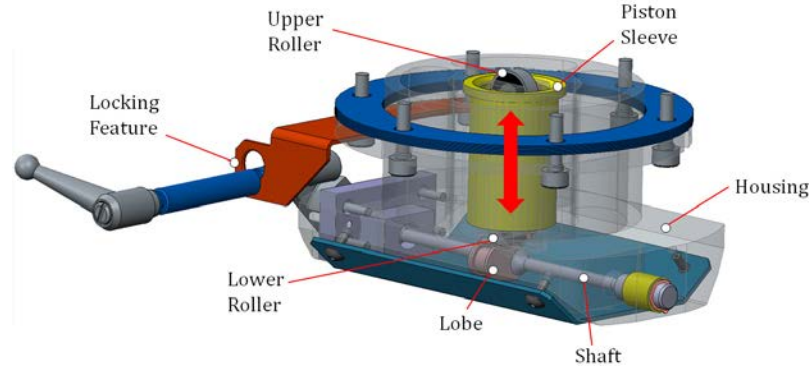


Figure 12. Cam over pre-load device used to repeatedly lock the position of the boom when it is extended.

A prototype system of the telescoping boom described above has been built and successfully tested. During the testing phase a few areas requiring improvements were determined and upgraded for the final design, such as the alignment of the bearings, inadequate rail constraints when retracting the boom, stiffness of load bearing members and ease of assembly. To perform alignment of the boom extension and desired preload on the rails the bearing packs are shimmed top and bottom using an array of shim stock. It was noted during the initial testing the array of varying thickness shims were too few and the fastening method too tedious. For the final configuration the mounting type has been updated to include a fixed pem-nut for ease of installation and wider range of shim stock to obtain the desired bearing locations. Additionally the prototype system did not include the upper forward most bearing pack that allowed for an unexpected freedom of motion as the boom was being retracted and extended. The upper most forward guide roller set is shimmed such that it does not apply any external force to the top rail when the boom is preloaded in the extended position. This bearing set only comes into play when the preload mechanism has been released and the boom is being moved. The boom in the prototype case was a thin walled rectangular box tube that induced an undesirable yaw error due to the sidewalls deforming while under load. The corrective action for this was to use a round cross-section and thicker material wall for the boom. Lastly the box structure that supports the boom was updated to include additional strong backs to further reduce deflection due to gravity. The preliminary results of the initial repeatability testing are shown below in Table 1.

Test performed with box tube cantilevered from cart			
trial	x error	y error	uRad
Vertical		Horizontal	
1	4.0	3.7	
2	4.0	15.7	
3	0.0	-4.3	
4	4.0	7.7	
5	-4.0	-0.3	
6	4.0	-4.3	
7	4.0	3.7	
8	-4.0	-4.3	
9	0.0	7.7	
10	-4.0	11.7	
11	-12.0	-12.3	
12	4.0	-24.3	

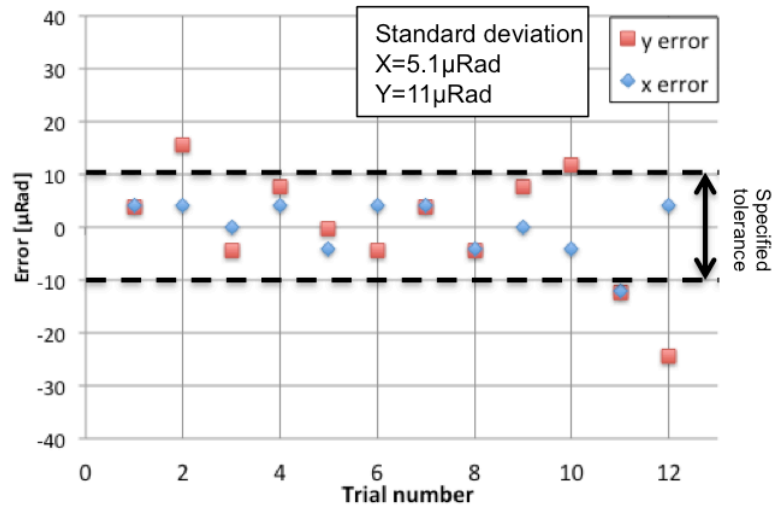


Table 1. Preliminary test results for the prototype and test of the telescoping boom. Further reductions in error are expected with the final configuration.

3.3.3 Full snout build

After the alignment of each quad and the co-alignment of all four channels have been verified the next step in the alignment process is the alignment of the DLP, which includes the boom, mirror pack assembly, a cross over block (Figure 13) and rear fiducial set on the cart station (Figure 14). The first step of this process is to mount the gated imager in the DIM cart and align it to the cart axis. Next, the telescoping boom is attached to the detector and aligned to within 0.5 mm using a combination of shimming the bearings and the mounting clearance on the bearing blocks. Auto collimating off the master target used on the CMM performs this step of the alignment process. Once the boom has been coarsely aligned the precise pointing of the boom is achieved by adjusting the gimbal and the translation stage. After the completion of this step the master target is removed and the crossover block is aligned.

The requirements for the KBO x-ray microscope point approach the limitations of the DIM alignment systems, Chamber Interior Viewing System (CIVS) and the Opposed Port Alignment System (OPAS) capabilities. To ensure the correct alignment of the KBO x-ray microscope a detailed error budget was created and assessed. The objective of the alignment process is to point the KBO quads optic axis through the desired aim point at the correct standoff distance.

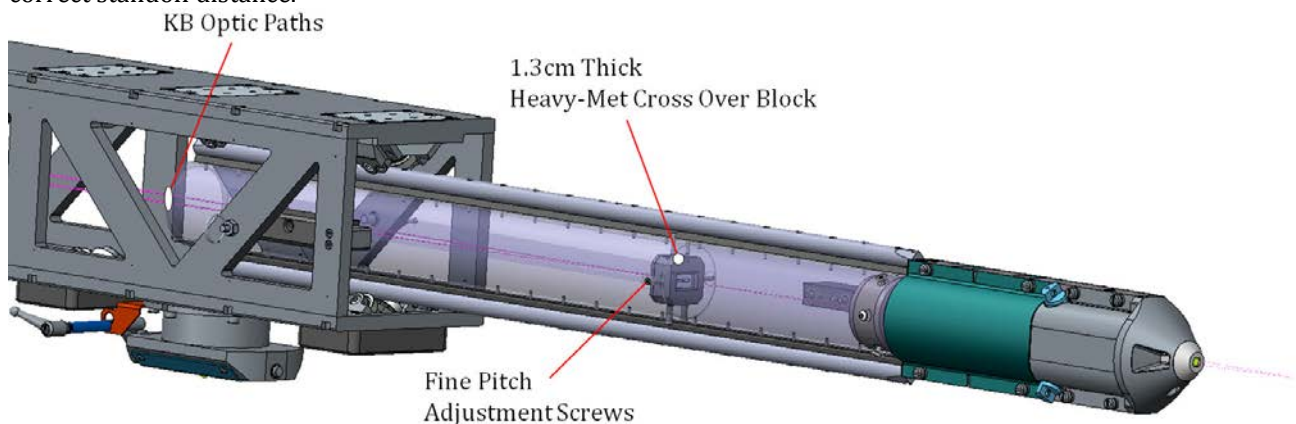


Figure 13. Location of heavy-met cross over block inside the KBO system boom.

Midway in the boom a 1.3 cm thick heavy-met crossover block is located where the four KBO images cross, shown in Figure 13. The crossover block is suspended in the center of the boom and is adjusted to the detector axis by an assortment of fine pitch adjustment screws, Figure 15. The rear OPAS fiducial set, shown in Figure 14, is then adjusted using the same technique, Figure 16. Lastly the pre-aligned mirror pack assembly, which includes the pinhole set, OPAS targets and mirror quads are installed.

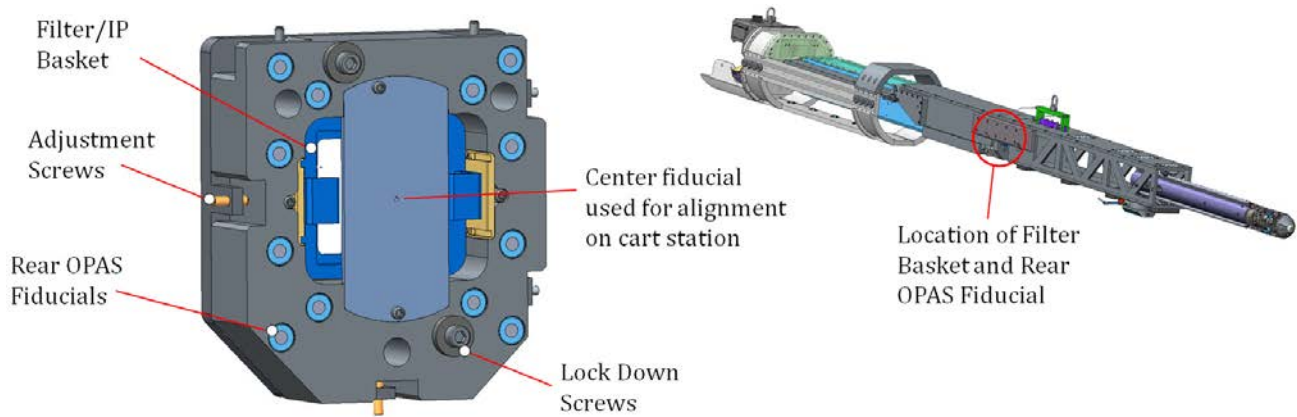


Figure 14. OPAS rear fiducial set is aligned using fine pitch adjustment screws to place it on the same centroid defined by the front set of targets.

3.4 Alignment to the experimental target on NIF: Utilization of the OPAS and CIVS systems

The rear and front fiducials are visible on the opposed port alignment system (OPAS) which has a resolution of $\sim 40 \mu\text{m}$. The central locations of these fiducials lie on a circle, the centroid of which is at a known location with respect to the cart axis. The centroid locations are defined at the front and rear of the DLP which allows the DIM to accurately position the DLP on a radial line of sight through target chamber center. The DLP is aimed by driving the bi-pods and pitching the DLP about the DIM gimbal which is located at the target chamber wall ~ 5.6 m from TCC. The insertion depth of the diagnostic is controlled by the CIVS system, which looks down at a fiducial placed on the spar of the debris shield. This system can resolve the snout position to $\sim 300 \mu\text{m}$ insertion distance of the diagnostic to target standoff.

Optical alignment of the mirror pack is tested extensively using an offline source that allows calibration of the diagnostic prior to fielding¹². Contributing to the alignment error of the diagnostic is the uncertainty that the cart station axis is parallel to the optical axis of the imaging system. An offset between these axes results in a systematic error in placement that could be removed with an alignment shot on NIF, if this shot can successfully decouple the image center from the requested pointing of the diagnostic. Due to the resolution following a coma response, imaging a grid with fiducials in NIF can perform this alignment experiment.

3.5 Alignment Summary

A high level summary of the required alignment and aim point to achieve the desired object spatial resolution of $\leq 8 \mu\text{m}$ is shown below in Table 2.

High-Level Contributions to alignment	Largest contributing factors	Tolerance Specification	Total effect on resolution at edge of 100 μ m diameter object (1 Sigma RMS)
Mirror pack alignment	Delivered Mirror radius of curvature	3.33mm	0.846 μ m
	Delivered asphere of mirror	1.33mm	
	Mirror Pitch Angle on CMM	$\pm 80\mu$ Rad	
	Translation of quad to center axis on CMM	$\pm 2\mu$ m	
	Front aperture location on CMM	$\pm 5\mu$ m	
NIF target chamber alignment	OPAS Alignment in TC	50 μ m	<3 μ m Equivalent to ± 0.049 mm pointing accuracy
	CIVS TCC to KB fiducial uncertainty	0.228mm	
	Boom Repeatability (Angle)	20 μ Rad	
	Insertion of DIM	0.2mm	
	Alignment shot correction factor	11 μ m	

Table 2. High-level alignment tolerances for the KBO x-ray microscope. Cart station alignment is not included as an alignment shot is planned that will measure the error introduced at that stage and effectively correct for it. Perfect alignment of the diagnostic would result in 5 μ m resolution at the edge of the 100 μ m object.

4. FIELDING THE KBO ON NIF

4.1 Debris Protection

The NIF lasers generate up to 2.0 MJ of laser energy to compress the target capsule. As the lasers interact with the target it generates a high velocity debris wind that would irreparably damage the KBO optics if they were not protected.

To protect the vital components of the x-ray microscope, exterior shielding and a replaceable debris window have been developed that can be easily exchanged between shots, shown in Figure 15. The design of the debris window was bounded by multiple constraints: the necessary clearance from laser beam paths, the expected debris wind loading and the limited access for exchange once loaded in the DIM.

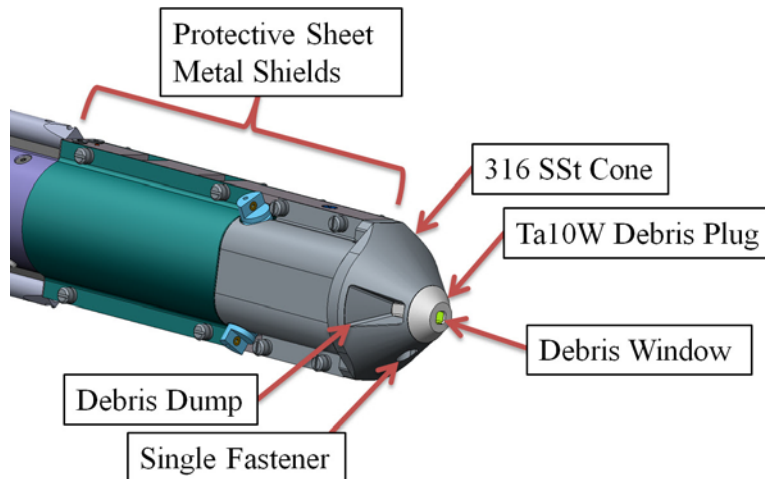


Figure 15. KBO front-end snout, shields, cone and replaceable debris plug assembly with sacrificial debris window.

Within the debris plug there are three primary components, the first of these components, indicated in the cross section shown in Figure 16, being a 25 μ m thick black Kapton x-ray ablative shield tilted at 45° to the axis of the snout. Normal to the x-ray ablative shield is an exit aperture (also referred to as a debris dump) for energy to escape or be diverted away from the primary sacrificial window. The sacrificial window is a 1.4 mm thick piece of polycarbonate which was the material of choice for the KBO because of its well-known x-ray transmission properties and its ability to withstand high velocity projectiles. Especially the latter made it an ideal candidate for computer simulations. Multiple of such simulations ¹⁴ were carried out to optimize the final design.

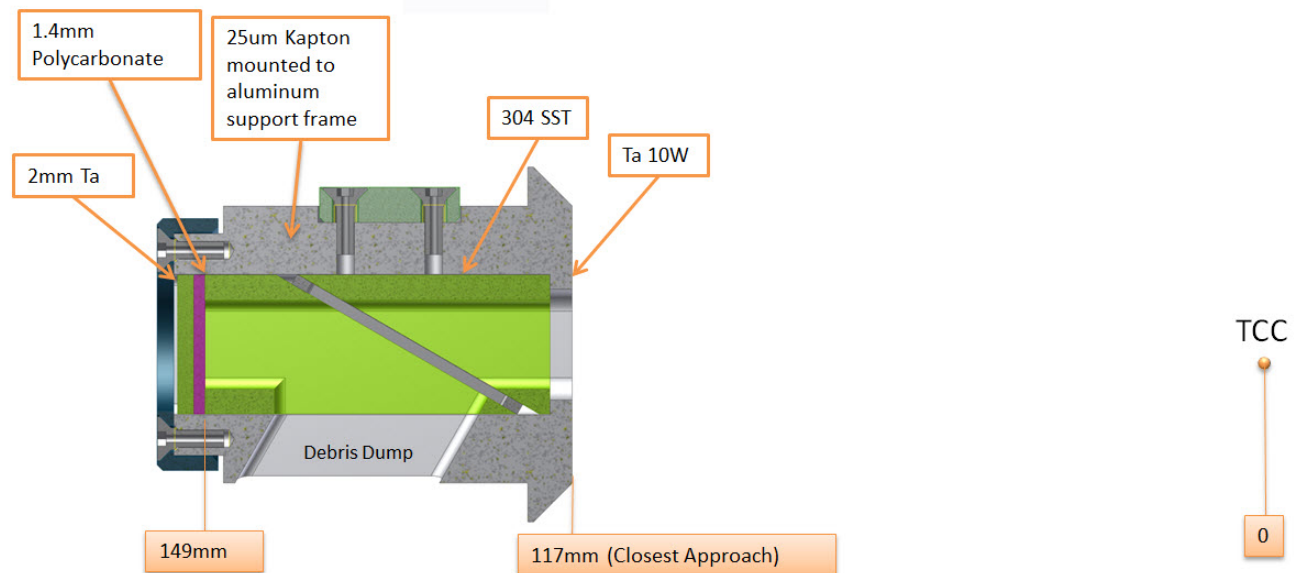


Figure 16. Cross-section view of the KBO debris plug. Listed are the materials and nominal standoff distances away from target chamber center (TCC)

For the simulation the vaporized mass of the target is assumed to be a spherically expanding shell of finite thickness traveling at approximately 100,000 m/s, with a loading duration on the exposed surface of approximately 3 μ s. The expanding shell is anisotropic, with the vertical loading being approximately 2x higher than the lateral loading, primarily driven by the direction and geometry of the target Hohlraum. The exact strength and direction of debris is target dependent with targets that are not fully vaporized posing a larger

threat of damaging the diagnostic and optics. Peak pressures in the lateral direction of approximately 1 GPa are typical for distances of 110 mm from the target. The results of modeling the effect of the expected debris wind on the debris plug design are shown in Figure 17.

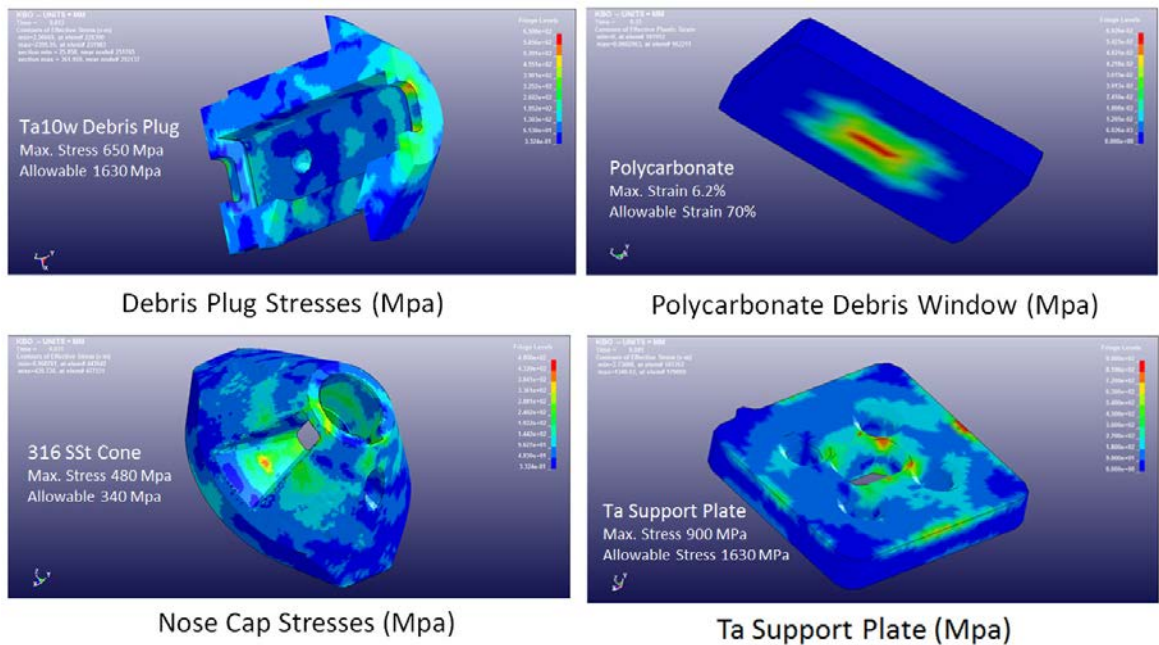


Figure 17. Sample simulations for the front cone and debris plug components nearest TCC when subjected to the resultant debris wind load generated from 2.0 MJ laser energy. Simulations were used to predict engineered safety margins for mirror protection and re-use of some components.

The forward most 25 μm thick black Kapton is completely vaporized when loaded with the debris wind and a significant amount of energy is diverted out the debris dump, thereby reducing the total load subjected onto the polycarbonate debris shield at the rear of the plug. To prevent the polycarbonate from fracturing a tantalum support plate is located behind it limiting the amount of polycarbonate deflection. The debris window is a replaceable unit that is housed inside a high strength alloy plug. The high strength plug material has exceptional elongation properties able to withstand repeated impact from high velocity target debris. For the purpose of the KBO the debris plug material chosen was Ta10W, a high strength tantalum tungsten alloy.

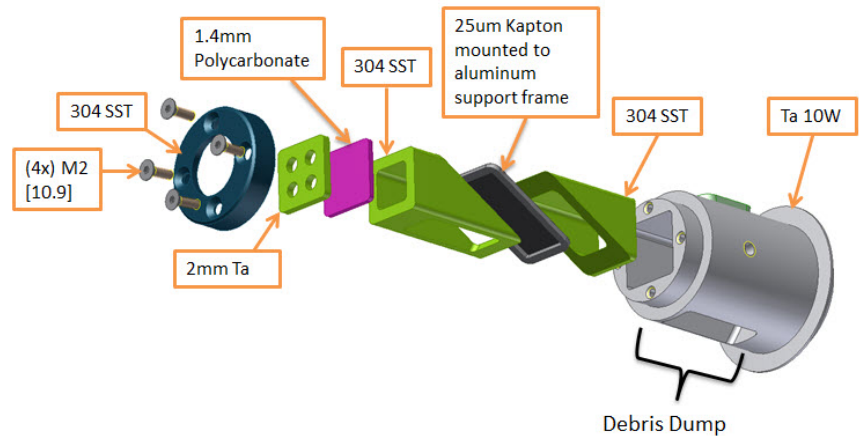


Figure 18. Exploded view of the KBO debris plug. Components are loaded into the back of the debris plug housing and then held in place by the rear cover. Typical consumable consists of only a 1.4 mm thick polycarbonate window.

An exploded view of the KBO debris plug is shown in Figure 18. The debris plug assembly is built off line and is designed for ease of replacement while the KBO system is still loaded in the DIM. Exchange of the debris plug requires simple venting of the DIM and the removal of one fastener. The design of the debris plug not only enables efficient operations but also reduces the amount of radiation exposure to the target area operators.

Assembly of the debris plug is a straightforward process wherein the components are stacked inside the debris plug housing and then pre-loaded by the rear cover plate. An integral key-feature and matching key-way in the cone ensure proper clocking of the debris plug components and for the four KBO apertures in the Ta support plate. Post-shot the used debris plug is disassembled, inspected for damage, and the polycarbonate window changed. The design intent of the debris plug is to reuse all components except for the polycarbonate window. Although not changed every shot the structural components will eventually see degradation from continuous use and will be noted during the post-inspection and replaced as needed.

The debris plug design allows the facility to maintain a high shot rate whilst providing more than sufficient protection to the mirrors from the NIF debris wind. Future iterations will allow the x-ray transmission properties of the plug to be varied to allow low energy application applying the same target specific debris wind analysis.

5. SUMMARY

The deployment of the new KBO x-ray microscope on NIF will provide improved spatial resolution, higher throughput and the ability for chromatic selection that is currently unavailable using standard pinhole framing camera technology. The remaining fabrication and build of the KBO-DLP is currently in process. Future plans will extend the number of available mirror packs to include a low energy broadband response and a narrow band 'high' energy coating, 16 keV, for radiographic applications. The box tubing will also be modified in future iterations to allow a film readout making the diagnostic compatible with high yield shots.

This work was performed by Lawrence Livermore National Laboratory under Contract No. DE-AC52-07NA27344

REFERENCES

- [1] G.A. Kyrala, S. Dixit, S. Glenzer, D. Kalantar et al., Rev. Sci. Instrum. **81** 10E316 (2010).
- [2] E. I. Moses *et al.*, Phys. Plasmas **16**, 041006 (2009).
- [3] P. Kirkpatrick and A. V. Baez, J. Opt. Soc. Am. **38**(9), 766–773 (1948).
- [4] R. H. Price and W. C. Friedhorsky, Report No. UCID-19831, 1983.
- [5] F. J. Marshall and Q. Su, Rev. Sci. Instrum. **66**(1), 725–727 (1995).
- [6] O. V. Gotchev, Rev. Sci. Instrum. **74**(12), 5065–5069 (2003).
- [7] J. F. Seely *et al.*, Appl. Opt. **35**, 4408 (1996).
- [8] T. Pardini *et al.*, Proc. SPIE **8850**, 88500E (2013).
- [9] N. Izumi *et al.*, Rev. Sci. Instrum. **81** 10E515 (2010).
- [10] D. Kalantar., *et al.*, Proc. SPIE **8505**, (2012).
- [11] M. D. Wilke *et al.*, Rev. Sci. Instrum. **79** 10E529 (2008).
- [12] L. A. Pickworth *et al.*, Rev. Sci. Instrum. **85**, 11D611 (2014).
- [13] W. J. Hibbard *et al.*, Rev. Sci. Instrum. **72**, 530 (2001).
- [14] Nathan D. Masters, NIF Debris Wind Worksheet – Rev B” Excel spreadsheet (NIF-5043393)